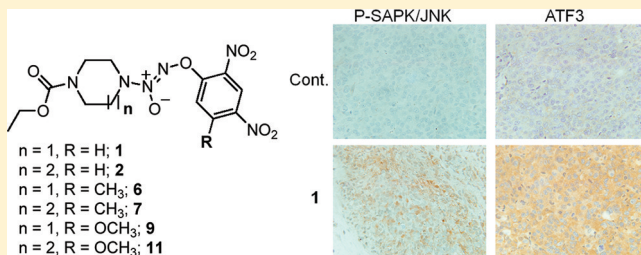# Activation of the c-Jun N-terminal Kinase/Activating Transcription Factor 3 (ATF3) Pathway Characterizes Effective Arylated Diazeniumdiolate-Based Nitric Oxide-Releasing Anticancer Prodrugs

Anna E. Maciag,[†,#,*] Rahul S. Nandurdikar,[‡,#] Sam Y. Hong,[‡] Harinath Chakrapani,[§] Bhalchandra Diwan,[†] Nicole L. Morris,[∥] Paul J. Shami,[⊥] Yih-Horng Shiao,[‡] Lucy M. Anderson,[‡] Larry K. Keefer,[‡] and Joseph E. Saavedra[†]

[†]Basic Science Program, SAIC-Frederick, Inc., National Cancer Institute, Frederick, Maryland 21702, United States

[‡]Chemical Biology Laboratory, National Cancer Institute, Frederick, Maryland 21702, United States

[§]Department of Chemistry, Indian Institute of Science Education and Research, Pune 411008, India

[∥]Laboratory Animal Sciences Program, SAIC-Frederick, Inc., National Cancer Institute, Frederick, Maryland 21702, United States

[⊥]Division of Hematology and Hematologic Malignancies, Huntsman Cancer Institute, University of Utah, Salt Lake City, Utah 84112, United States

Ⓢ *Supporting Information*

ABSTRACT: Improved therapies are needed for nonsmall cell lung cancer. Diazeniumdiolate-based nitric oxide (NO)-releasing prodrugs are a growing class of promising NO-based therapeutics. Recently, we have shown that O^2-(2,4-dinitrophenyl) 1-[(4-ethoxycarbonyl)piperazin-1-yl]diazen-1-ium-1,2-diolate (JS-K, **1**) is effective against nonsmall cell lung cancer (NSCLC) cells in culture and in vivo. Here we report mechanistic studies with compound **1** and its homopiperazine analogue and structural modification of these into more stable prodrugs. Compound **1** and its homopiperazine analogue were potent cytotoxic agents against NSCLC cells in vitro and in vivo, concomitant with activation of the SAPK/JNK stress pathway and upregulation of its downstream effector ATF3. Apoptosis followed these events. An aryl-substituted analogue, despite extended half-life in the presence of glutathione, did not activate JNK or have antitumor activity. The data suggest that rate of reactivity with glutathione and activation of JNK/ATF3 are determinants of cancer cell killing by these prodrugs.

n = 1, R = H; **1**
n = 2, R = H; **2**
n = 1, R = CH₃; **6**
n = 2, R = CH₃; **7**
n = 1, R = OCH₃; **9**
n = 2, R = OCH₃; **11**

P-SAPK/JNK   ATF3   Cont.   **1**

INTRODUCTION

Lung cancer is a leading cause of cancer deaths worldwide. Nonsmall cell lung cancer (NSCLC) accounts for about 80% of all lung cancers. Despite recent advances in therapy, the disease remains largely incurable. For patients with advanced disease, current platinum-based chemotherapy regimens result in median survival of 7−10 months only.[1]

O^2-(2,4-Dinitrophenyl) 1-[(4-ethoxycarbonyl)piperazin-1-yl]diazeniumdiolate (**1**, JS-K) has proven effective in several in vivo cancer models.[2−5] Recently, we have shown that **1** is effective against NSCLC cells in vitro and in vivo.[6] The mechanism(s) of action of **1** is only partially understood. The drug appears to have a multifaceted cell-type-dependent mode of action with NO-mediated pathways and S-arylation of cellular thiols being involved. In NSCLC cells, its effectiveness depends on endogenous reactive oxygen species (ROS): the compound was most effective in cell lines characterized by high levels of endogenous ROS. The toxic effects involved mitochondrially mediated apoptosis via caspase-dependent mechanisms and were independent of the p53 tumor suppressor status. DNA strand-break damage measured by comet assay was also observed.[6] Similarly, in multiple myeloma cells, **1** caused DNA double strand break damage.[5]

Compound **1** and its analogues release nitric oxide (NO) on reaction with glutathione (GSH) (Scheme 1), and this reaction is accelerated by glutathione *S*-transferases (GST).[7] We have previously shown that a homopiperazine analogue of **1**, compound **2** (Scheme 1), is less reactive than **1** with GST and exhibits an extended half-life in the presence of GSH in comparison to the parent drug in vitro.[7] We hypothesized that this property of the drug might translate to a prolonged lifetime in the bloodstream and selective accumulation of the drug in the tumor, thus leading to better antitumor efficacy.

In an attempt to create more stable analogues, we have synthesized a small library of compounds by substituting the C5-position of the aryl ring of the parent compounds with methyl or methoxy groups to make the resulting compounds

Scheme 1. Mechanism of Nitric Oxide Release from 1 and Its Homopiperazine Analogue 2
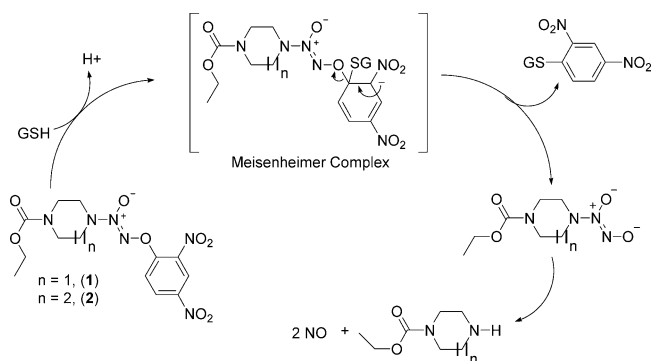
more resistant to glutathione/GST attack and thereby extending their half-lives in the reaction with GSH. The second-generation compounds were screened in vitro against a panel of NSCLC cell lines, and the most promising prodrugs were tested in vivo in an H1703 nonsmall cell lung cancer xenograft model. We show that the homopiperazine analogue of 1, compound 2, exhibits almost identical in vitro activity as the parent drug. However, its in vivo efficacy appears to be more pronounced. Substitution of the C5-position in the aryl ring with a methyl group led to diminished reactivity of the compound toward glutathione. However, this analogue did not exhibit any antitumor efficacy in vivo. The reasons for this difference were sought. Both 1 and 2 caused rapid and sustained activation of the SAPK/JNK stress pathway in NSCLC cells in culture and in vivo as well as significant cell death in xenografted tumors. In contrast, O^2-(2,4-dinitro-5-anisyl) and O^2-(2,4-dinitro-5-tolyl) analogues did not cause SAPK/JNK pathway activation and histochemical analysis did not reveal cell death in the tumors from animals treated with O^2-(2,4-dinitro-5-tolyl) analogue. We conclude that SAPK/JNK pathway activation is important for this class of compounds to induce tumor cell death in vivo.

■ RESULTS

Synthesis. 1 and its homopiperazine analogue 2 (Scheme 1) were synthesized following the reported procedures.[3,8] Syntheses of the tolyl and anisyl analogues are shown in Scheme 2. Reactions of diazeniumdiolate sodium salts 3 and 4

with 2,4-dinitro-5-fluorotoluene (5) in DMSO at room temperature furnished the tolyl analogues 6 and 7, respectively, in good yields. Synthesis of the anisyl analogue 9 began with the reported compound 8.[3] Nucleophilic displacement of the fluorine with methoxide ion in compound 8 was accomplished using sodium methoxide in methanol to obtain the desired anisyl compound 9 in 51% yield. An alternate strategy was used for the synthesis of the homopiperazine anisyl analogue 11. Diazeniumdiolate sodium salt 4 was treated with 2,4-dinitro-5-fluoroanisole (10)[9] in 5% NaHCO₃ in ʹBuOH:THF to afford the desired compound 11 in 63% yield.

Decomposition Studies and Nitric Oxide Release. The rates of reaction of 1 and its analogues with 4 mM glutathione (GSH) in aqueous pH 7.4 phosphate buffered saline at 37 °C were determined (Table 1). The results show that substituting

Table 1. Stability of the Compounds in the Presence of 4 mM GSH, and in Vitro Antiproliferative Activities

compd	$t_{1/2}$(min) mean (SE)	IC₅₀ (μM)				
		H1703	H441	H1373	H2122	H1944
1	15.7 (1.4)	0.57	0.94	0.86	3.17	>10
2	22.6 (0.4)	0.64	1.42	0.95	3.14	>10
6	71.5 (4.3)	0.97	1.61	1.86	7.00	>10
7	25.7 (1.0)	1.66	2.02	3.00	10.0	>10
9	38.6 (2.8)	1.57	2.50	2.10	5.78	>10
11	59.6 (4.2)	1.82	3.15	3.08	10.0	>10

the phenyl ring with tolyl or anisyl rings significantly increased the half-life of the reaction with 4 mM GSH (Table 1). Replacing the piperazine moiety of 1 with homopiperazine also resulted in a more stable compound (2). The decomposition showed pseudofirst-order kinetics. To illustrate this, the plot for the decomposition for compound 6 is shown in Supporting Information Figure S1. We have previously reported this phenomenon and shown that this analogue has diminished reactivity with GST.[7]

In Vitro Efficacy. In a previous study,[6] we screened a panel of 18 NSCLC cell lines for sensitivity to 1. Compound 1 inhibited growth of all NSCLC cell lines with IC₅₀ concentrations ranging from 0.33 to 17.64 μM. Six cell lines were inhibited in the range of 0.33 to 1.01 μM and were thus as sensitive as leukemia cells[2] or multiple myeloma cells.[5] In this

Scheme 2. Synthesis of the Tolyl and Anisyl Analogues of 1 and 2
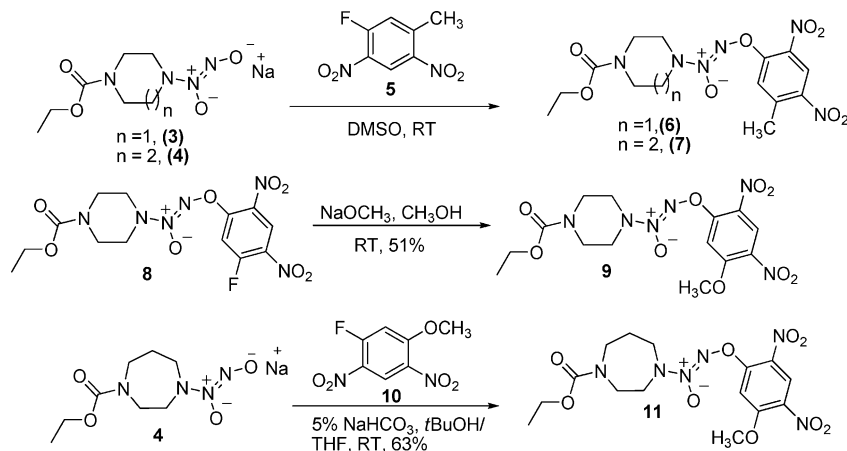
work, we have chosen three **1**-sensitive cell lines (H1703, H441, and H1373) and two significantly less sensitive lines (H2122 and H1944) for evaluation of growth-inhibitory activities of the new analogues. The results are given in Table 1. Compounds **1** and **2** exhibited very comparable antiproliferative activities against the NSCLC cell lines (Table 1). This finding is consistent with our previous comparison of anticancer activities of **1** and **2** against a larger panel of cancer cell lines from different sites.[7] Surprisingly, increased stability of **6**, **9**, and **11** in the presence of glutathione did not result in increased toxicity against cancer cells in culture.

In Vivo Studies. NSCLC cell line H1703, with established in vivo sensitivity to **1**,[6] was chosen for assessment of activity of the prodrugs in vivo against xenografted cells in athymic mice. To compare the effects of prolonging the half-life of the compound on the in vivo efficacy, compounds **2** and **6** were chosen for further studies. The compounds were formulated in Pluronic P123. Compounds **1** and **2** were administered at 6 μmol/kg. Compound **6**, which is significantly more stable to nucleophilic attack by GSH, was delivered at 8 μmol/kg. The drugs were administered intravenously, three times a week for a 3-week period, to assess anticancer activity. Treatment with either **1** or **2** significantly reduced growth of H1703 human NSCLC cells when compared with cells in control animals treated with vehicle only. Despite the higher dosage of **6**, treatment did not result in reduction in H1703 tumor growth in vivo. Figure 1 shows a comparison of the tumor weights from
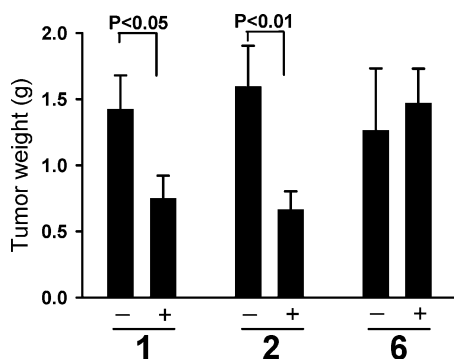

Figure 1. H1703 cells growth in vivo was significantly inhibited by **1** or **2** but not by **6**. Compounds **1** and **2** were administered iv at 6 μmol/kg and compound **6** at 8 μmol/kg. The injections were performed three times a week for three weeks. Growth of tumors treated with **1** or **2** was inhibited, in contrast to **6**, for which tumor weights did not differ significantly from the controls. Values are means ± SE (Mann–Whitney test); numbers of mice for the control and treated groups, respectively, were 13 and 14 for **1**, 14 and 15 for **2**, and 13 and 14 for **6**. The treatment did not affect body weights. The average body weights at the beginning of the experiment were 22.5 ± 0.4 g, 22.5 ± 0.4 g, and 22.2 ± 0.4 g for groups **1**, **2** and **6**, respectively. At the end of the treatment, the weights were: in group **1**, 24.6 ± 0.9 g and 24.9 ± 0.4 g; in group **2**, 24.6 ± 0.6 g and 24.9 ± 0.4 g; and in group **6**, 24.6 ± 0.6 g and 24.5 ± 0.6 g, vehicle control and compound-treated, respectively.

drug-treated animals relative to vehicle-treated controls at the termination of the experiment. Treatment with **1** led to 49% reduction of the tumor weights ($P < 0.05$). Treatment with **2** resulted in 63% reduction of the tumor weights ($P < 0.01$). Importantly, treatment with either vehicle or diazeniumdiolate-based drugs did not affect body weights (see legend to Figure 1).

Activation of a SAPK/JNK Stress Pathway. We have shown previously that treatment with **1** resulted in oxidative/nitrosative stress and DNA damage in H1703 cells.[6] Both oxidative stress and DNA damage are widely observed to activate a SAPK/JNK pathway, leading to activation of transcription factors and expression of stress-response genes. It has been documented that SAPK/JNK activation is necessary for apoptosis induced by various stress stimuli in several cell types.[10,11]

Treatment of H1703 cells with 1 μM compound **1** resulted in rapid phosphorylation of SAPK/JNK (through its upstream kinase SEK1/MKK4) and its downstream effectors, transcription factors ATF2 and c-jun, and in increased activating transcription factor 3 (ATF3) protein (Figure 2A). Phosphorylation of SAPK/JNK was detected within 30 min of treatment. Activation of ATF2 and c-jun was inhibited by pretreatment with JNK inhibitor 1,9-pyrazoloanthrone (Figure 2B). Only **1** or **2** caused SAPK/JNK activation; treatment with the other four compounds did not lead to SAPK/JNK phosphorylation (Figure 2C).

Preincubation of the H1703 cells with ROS scavenger Tiron attenuated SAPK/JNK phosphorylation resulting from **1** or **2** (Figure 2D), which suggests activation of the pathway by oxidative stress. As a loading control, membranes were reprobed with a SAPK/JNK antibody. No variation in the amount of SAPK/JNK protein was detected.

ATF3 may be strongly induced in a variety of tissues by different stress signals.[12] Several pathways, including JNK, could be responsible for ATF3 induction in a p53-dependent or -independent manner.[13,14] Accumulating evidence suggests that ATF3 plays a significant role in apoptosis. When overexpressed, ATF3 induced apoptosis in ovarian cancer cells[15] and sensitized HeLa cells to chemotherapy.[16] ATF3 was also shown to play a role in β-cell apoptosis.[14] In the present study, ATF3 protein expression was induced by 1 μM **1** or **2** within 2 h of the treatment (Figure 2A,E). Other analogues did not upregulate ATF3. ATF3 upregulation was partially blocked by pretreatment with 1,9-pyrazoloanthrone, which confirms that its activation was in part JNK-dependent (Figure 2B). Figure 2E shows a time course of ATF3 activation by **1** or **2** but not **6**. ATF3 was activated through an increase in mRNA. Real-time PCR (RT-PCR) analysis of ATF3 mRNA level revealed its rapid upregulation after treatment with **1**. We observed 8-fold increase in ATF3 mRNA level after 1.5 h treatment with 1 μM compound **1** and 10-fold increase with 5 μM **1** (Figure 2F).

Treatment with 1 or 2 Resulted in Arrest of the Cell Cycle in G2/M Phase and Commitment to Apoptosis. Treatment of H1703 cells with **1** or **2**, but not **6**, for 1, 4, or 6 h resulted in cleavage of PARP, a reliable indicator of apoptosis (Figure 3A). This was confirmed in a further experiment in which cleavage of caspases 3 and 7 were also measured (Figure 3B). A preliminary study utilizing fluorescence-activated cell sorting (FACS) further confirmed apoptosis and indicated G2/M growth arrest. After 6 h treatment with 1 μM **1**, 37% of H1703 cells were in the G2 phase and 14.4% were apoptotic. Control (DMSO-treated) H1703 cells processed in parallel exhibited 8% in G2 phase and 0.05% cells found to be apoptotic.

Silencing of ATF3 Prevents 1-Induced Apoptosis. The H1703 cells were treated with siRNA to ATF3 for 48 h, followed by treatment with compound **1** or DMSO (control) for 8 h. In the cells pretreated with siRNA to ATF3, treatment with **1** did not result in upregulation of ATF3 protein
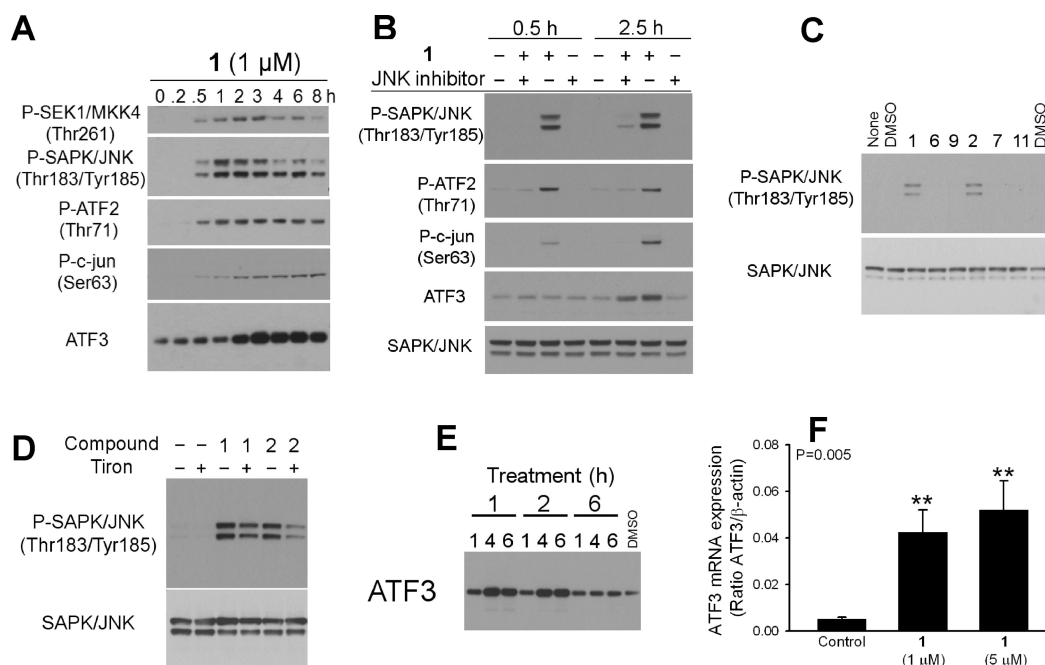
Figure 2. Only **1** and **2** activated the SAPK/JNK stress pathway in H1703 cells. Representative blots are shown. (A) Activation of SAPK/JNK and its downstream effectors upon **1** treatment. (B) Pretreatment of the H1703 cells with 1,9-pyrazoloanthrone (50 μM, 30 min) inhibited **1**-induced phosphorylation of JNK and its downstream effectors ATF2 and c-jun. Blocked upregulation of ATF3 protein confirms that its activation was in part JNK-dependent. (C) Only **1** and **2** induced JNK phosphorylation. (D) Pretreatment with ROS scavenger Tiron partially blocked JNK activation by **1** or **2**. Cells were pretreated with 10 mM Tiron for 1 h, followed by 30 min incubation with **1** or **2**. (E) ATF3 protein expression was induced by **1** or **2** but not by **6**. H1703 cells were treated with 1 μM compound or DMSO for 1, 4, or 6 h, then lysed and processed by Western blotting for ATF3 protein. (F) ATF3 mRNA levels in H1703 cells treated with **1** were evaluated by quantitative RT-PCR. β-actin was used as an internal control. Data are reported as mean ± SE.
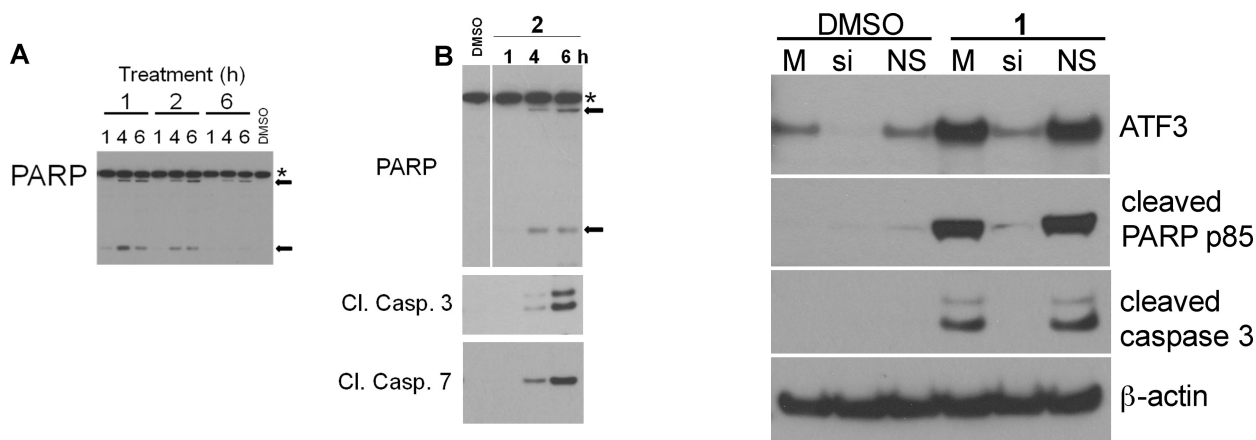

Figure 3. Activation of apoptosis as evidenced by PARP cleavage and activation of effector caspases 3 and 7. (A) H1703 cells were treated with 1 μM compound or DMSO for 1, 4, or 6 h, then lysed and processed by Western blotting for PARP protein. PARP cleavage was induced by **1** and **2** but not by **6**. (B) Cells were treated with 1 μM **2** for the time periods indicated or DMSO for 6 h. Stars indicate full-length PARP (116 kDa), and arrows indicate cleaved fragments (89 and 24 kDa).

Figure 4. Silencing of ATF3 protects from **1**-induced apoptosis. H1703 cells were treated with siRNA to ATF3 or controls for 48 h, followed by treatment with 1 μM compound **1** or DMSO (control) for 8 h, then lysed and processed for Western blotting for cleaved PARP p85 and cleaved caspase 3 proteins. β-actin was used as a loading control. M, mock (reagent control); si, siRNA to ATF3; NS, nonsilencing siRNA control.

expression (Figure 4). Activation of apoptosis was also inhibited: in the cells pretreated with siRNA to ATF3, induction of apoptosis resulting from treatment with **1** was inhibited, as evidenced by lack of cleaved PARP signal and cleaved caspase-3 signal (Figure 4). Control cells (reagent-control or nonsilencing control treated) responded to the treatment with strong apoptotic signals. This strongly suggests

that ATF3 is involved in induction of apoptosis in H1703 cells after treatment with **1**.

SAPK/JNK Activation and ATF3 Upregulation is Also Observed in Xenograft Tumors. Next, we investigated if these differences in activating JNK pathway could be observed in vivo, in xenograft tumors. H&E staining analysis revealed significant tissue death in **1**- or **2**-treated tumors, in contrast to the tumors from animals treated with compound **6** or vehicle

control (Figure 5). Immunohistochemical analysis of the tumors revealed phosphorylation of SAPK/JNK, as well as
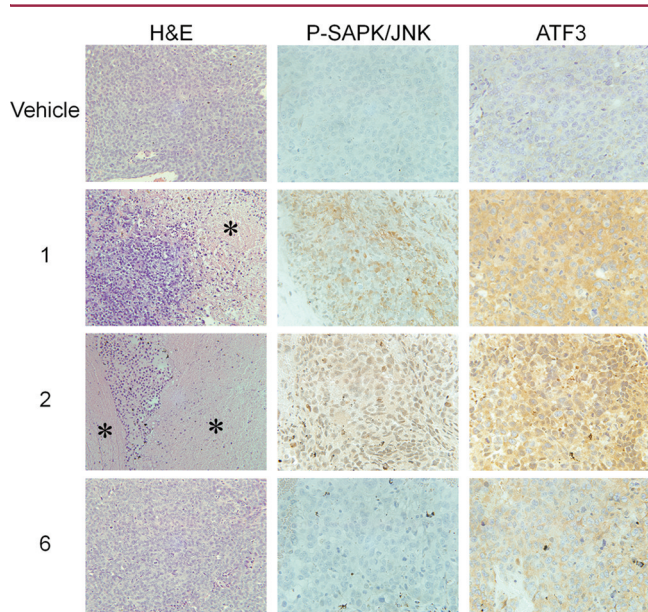

Figure 5. H&E staining shows significant areas of cell death (stars) in tumors from animals treated with **1** or **2** in contrast to **6** or vehicle-treated controls. Tumors treated with **1** or **2** show strong staining for phosphorylated SAPK/JNK and ATF3. Controls or tumors treated with **6** show very weak staining. Representative tumors are shown.

upregulation in ATF3 protein level in the tumors treated with **1** or **2**. Tumors treated with vehicle control or **6** did not stain for P-SAPK/JNK, and the ATF3 signal was comparable to that of the control, much weaker than that resulting from the treatment with **1** or **2** (Figure 5, Supporting Information Table S2).

■ DISCUSSION

Lung cancer is one of the most common and deadly malignancies, and novel treatment strategies are urgently needed. In our previous report,[6] we correlated the anticancer activity of compound **1** against NSCLC cells with the endogenous levels of ROS/RNS. We reported multiple mechanisms playing a role in the drug's cytotoxicity, including depletion of glutathione, DNA damage, and MnSOD protein tyrosine nitration leading to mitochondrially mediated apoptosis.

Here we presented evidence that both **1** and its homopiperazine analogue **2** activated the SAPK/JNK stress signaling pathway, and this induction could be partially suppressed by a ROS scavenger. Involvement of the SAPK/JNK pathway in activation of apoptotic cell death has been reported,[10] as well as its involvement in ATF3 induction.[17] SAPK/JNK activation in response to **1** has been shown in hepatoma[4] and multiple myeloma cells.[5]

ATF3 can be greatly induced by cellular stress, including UV irradiation, ROS, or NO. Its induction often associates with cellular damage, suggesting an important role during stress response.[12,18,19] ATF3 upregulation can be mediated by ATF2, another member of the ATF/CREB family. Although ATF2 expression has been associated with maintaining a malignant phenotype, possible tumor suppressor functions also have been reported.[20] An increase in ATF3 expression in the treated cells as well as xenograft tumors is interesting for two reasons. First, ATF3 has been implicated in apoptosis,[14−16] which raises the possibility that this transcription factor is a novel mediator of the antitumor effects of **1** or **2**. Second, ATF3 has been reported to be induced by NO;[21] strong immunostaining of ATF3 in the tumors from animals treated with **1** or **2** suggests that the prodrugs are stable enough in the circulation to be able to deliver cytotoxic NO to the tumor.

Scheme 3. Proposed Cellular Mechanisms of NO Prodrug Toxicity
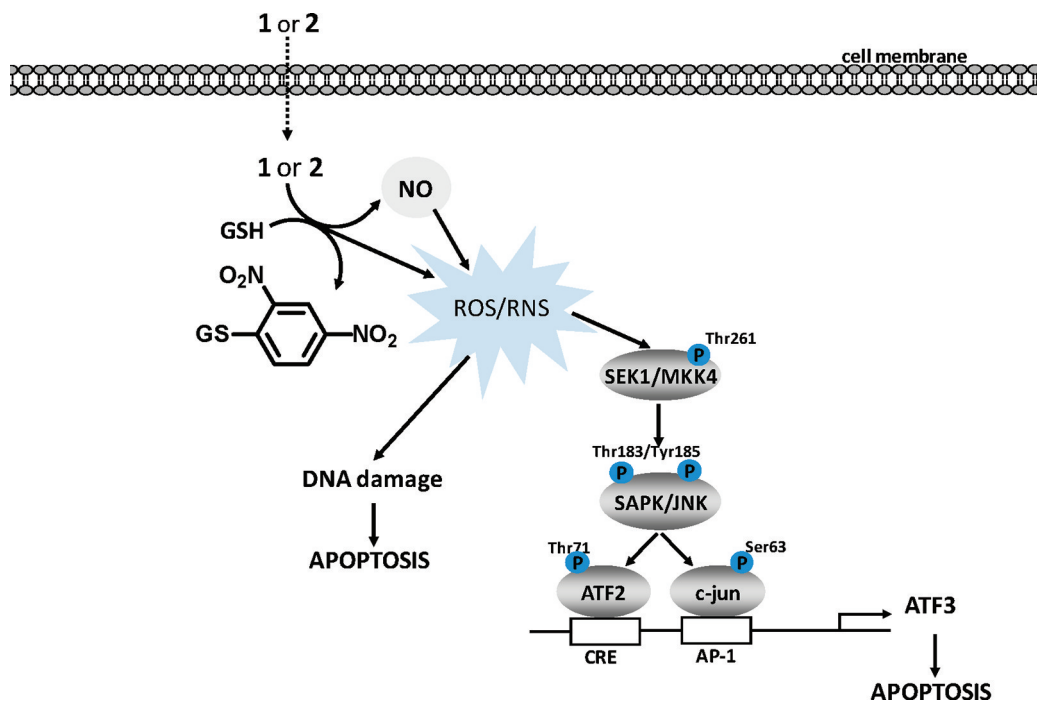
The methyl and methoxy substituents in compounds **6, 7, 9**, and **11** were introduced in order to increase the electron density at the carbon bearing the diazeniumdiolate moiety. Increased electron density would render these analogues less susceptible to nucleophilic attack and thus hamper rate-limiting formation of the Meisenheimer complex along with the subsequent elimination of the diazeniumdiolate anion. Indeed, this modification to the structure led to an increased half-life of the compounds, which did not, however, translate to increased antiproliferative activity. The substituted analogue lacked the ability to induce SAPK/JNK phosphorylation and ATF3 induction both in vitro and in vivo.

Our results suggest that rate of reactivity with GSH is a critical factor for the effectiveness of this class of compounds, perhaps due to increased ROS consequent to GSH depletion. An alternative explanation may be the fact that by being less reactive with GSH, **6** is less efficient in delivering NO (the primary toxin in these prodrugs) to the malignant cells (Scheme 3). Stereoelectronic perturbations associated with methyl and methoxy substitutions of the aromatic ring may also contribute to the observed differences in in vivo activity. Most likely, our observations are due to a combination of these factors.

■ EXPERIMENTAL SECTION

General. Starting materials were purchased from Aldrich Chemical Co. (Milwaukee, WI) unless otherwise indicated. 2,4-Dinitro-5-fluorotoluene was purchased from Oakwood Products, Inc., West Columbia, SC. NMR spectra were recorded on a Varian UNITY INOVA spectrometer; chemical shifts (δ) are reported in parts per million (ppm) downfield from tetramethylsilane. The NMR spectra of compounds **7** and **11** were recorded at 70 °C in DMSO-d_6. Ultraviolet (UV) spectra were recorded on an Agilent model 8453 or a Hewlett-Packard model 8451A diode array spectrophotometer. Elemental analyses were performed by Midwest Microlab (Indianapolis, IN). Chromatography was performed on a Biotage SP1 flash purification system. Prepacked silica gel flash chromatography columns were purchased from Silicycle (Quebec City, Canada). Compounds **1−4**[3], **8**[3], and **10**[9] were prepared using reported methods. All the new compounds were found to be >95% pure as determined by NMR, elemental analyses, and HPLC.

O^2-(2,4-Dinitro-5-methylphenyl) 1-[(4-Ethoxycarbonyl)-piperazin-1-yl]diazen-1-ium-1,2-diolate (6) (JS-55−111). A solution of **3** (543 mg, 2.5 mmol) in 10 mL of DMSO was stirred at room temperature. A solution of **5** (500 mg, 2.5 mmol) in 5 mL of DMSO was added through a syringe. The solution turned green upon addition and faded to yellow gradually. The solution was stirred at room temperature for 72 h, flooded with 25 mL of ice−water, and extracted with ether. The organic layer was dried over sodium sulfate and filtered through a layer of anhydrous magnesium sulfate. Evaporation of the solvent gave a yellow solid that was recrystallized from ether−petroleum ether to give compound **6** (409 mg). The aqueous/DMSO layer was allowed to stand overnight, producing an additional 181 mg of product **6** (total yield: 64%). mp 81−83 °C; UV (ethanol) λ_{max} (ε) 252 nm (12.2 mM^{-1} cm^{-1}), λ_{max} (ε) 290 nm (11.6 mM^{-1} cm^{-1}). ^{1}H NMR (CDCl$_3$) δ 1.29 (t, J = 7.0 Hz, 3H), 2.75 (s, 3H), 3.60−3.63 (m, 4H), 3.72−3.75 (m, 4H), 4.19 (q, J = 7.0 Hz, 2H) 7.44 (s, 1H), 8.78 (s, 1H). ^{13}C NMR (CDCl$_3$) δ 14.62, 21.61, 42.24, 50.68, 62.08, 120.70, 123.05, 123.85, 141.94, 151.89, 155.01. Anal. (C$_{14}$H$_{18}$N$_6$O$_8$) C, H, N.

O^2-(2,4-Dinitro-5-methylphenyl) 1-[(4-Ethoxycarbonyl)-homopiperazin-1-yl]diazen-1-ium-1,2-diolate (7) (RN-2−45). To a solution of **4** (254 mg, 1.0 mmol) in 5 mL of DMSO was added a solution of **5** (200 mg, 1.0 mmol) in 1 mL of DMSO at room temperature. After 12 h, reaction was quenched with ice−water and extracted with ether. The combined organic layer was dried over anhydrous sodium sulfate, and solvent was evaporated under reduced

pressure. The crude material was purified by flash column chromatography (1:1 hexane/ethyl acetate) to afford product **7** (190 mg, 46%) as a yellow solid. UV (ethanol) λ_{max} (ε) 304 nm (17.7 mM^{-1} cm^{-1}). ^{1}H NMR (DMSO-d_6, 70 °C) δ 1.09 (t, J = 7.0 Hz, 3H), 1.83−1.89 (m, 2H), 2.62 (s, 3H), 3.40 (t, J = 5.8 Hz, 2H), 3.64 (t, J = 5.9 Hz, 2H), 3.89 (t, J = 5.7 Hz, 2H), 3.95−4.00 (m, 4H), 7.60 (s, 1H), 8.66 (s, 1H). ^{13}C NMR (DMSO-d_6, 70 °C) δ 14.81, 20.88, 25.71, 44.17, 45.66, 50.25, 50.62, 61.25, 120.54, 123.68, 135.03, 142.39, 142.85, 151.90, 155.48. Anal. (C$_{15}$H$_{20}$N$_6$O$_8$) C, H, N.

O^2-(2,4-Dinitro-5-methoxyphenyl) 1-[(4-Ethoxycarbonyl)-piperazin-1-yl]diazen-1-ium-1,2-diolate (9) (JS-56−32). To a solution of **8** (246 mg, 0.612 mmol) in 10 mL of dichloromethane was added 5.4 M sodium methoxide in methanol (0.113 mL, 0.612 mmol). The resulting orange solution faded to a light yellow−orange solution. TLC analysis on silica gel using 10:1 dichloromethane:ethyl acetate indicated that all the starting material had reacted within the first 5 min of reaction. The solution was diluted with 25 mL of dichloromethane, washed with water, dried over sodium sulfate, filtered through a layer of anhydrous magnesium sulfate, and evaporated under vacuum to give 208 mg of a resin. The resin solidified upon trituration with ether, and the resulting yellow powder was collected by filtration giving product **10** (128 mg, 51%): mp 142−144 °C; UV (ethanol) λ_{max} (ε) 276 nm (10.2 mM^{-1} cm^{-1}). ^{1}H NMR (CDCl$_3$) δ 1.29 (t, J = 7.0 Hz, 3H) 3.57−3.62 (m, 4H), 3.72−3.75 (m, 4H), 4.09 (2, 3H), 4.19 (q, J = 7.0 Hz, 2H) 7.11 (s, 1H), 8.79 (s, 1H). ^{13}C NMR, (CDCl$_3$) δ 14.61, 42.20, 50.71, 57.54, 62.10, 101.52, 125.57, 154.21, 157.84, 165.87, 175.96. Anal. (C$_{14}$H$_{18}$N$_6$O$_9$) C, H, N.

O^2-(2,4-Dinitro-5-methoxyphenyl) 1-[(4-Ethoxycarbonyl)-homopiperazin-1-yl]diazen-1-ium-1,2-diolate (11) (RN-2−50). To a solution of **4** (254 mg, 1.0 mmol) in 5% sodium bicarbonate (8 mL) was added a solution of **10** (216 mg, 1.0 mmol) in 1:1 THF/tBuOH (8 mL) at room temperature. After 12 h, the reaction mixture was diluted with 15 mL of ether, and the organic layer was separated. The aqueous layer was extracted with ether (2 × 10 mL). The combined organic layer was dried over anhydrous sodium sulfate, and solvent was evaporated under reduced pressure. The crude material was purified by flash column chromatography (1:1 hexane/ethyl acetate) to afford product **11** (270 mg, 63%) as a yellow solid: UV (ethanol) λ_{max} (ε) 305 nm (14.1 mM^{-1} cm^{-1}). ^{1}H NMR (DMSO-d_6, 70 °C) δ 1.09 (t, J = 7.00 Hz, 3H), 1.88 (broad, 2H), 3.40 (t, J = 6.0 Hz, 2H), 3.65 (t, J = 5.4 Hz, 2H), 3.90 (t, J = 5.5 Hz, 2H), 3.94−4.01 (m, 4H), 4.06 (s, 3H), 7.29 (s, 1H), 8.68 (s, 1H). ^{13}C NMR (DMSO-d_6, 70 °C) δ 14.92, 25.54, 44.20, 45.59, 50.13, 50.56, 58.49, 61.28, 120.00, 125.28, 129.30, 133.03, 154.48, 157.90. Anal. (C$_{15}$H$_{20}$N$_6$O$_9$) C, H, N.

Formulated Prodrug Stability Studies. First, 490 μL of 2.25% Pluronic P123 in phosphate-buffered saline (PBS) was aliquoted into glass HPLC vials and maintained at 50 °C. To this solution, 10 μL of 50 mM prodrug in DMSO was added and maintained at 50 °C for 10 min. Then a glutathione stock solution (40 mM) was prepared in 0.1 M phosphate buffer, pH 7.4. To 800 μL of 0.1 M phosphate buffer in a glass HPLC vial, 100 μL of glutathione stock solution and 100 μL of formulated prodrug were added. The disappearance of the prodrug was monitored using an Agilent 1100 series HPLC fitted with a C-18 reverse phase column (Phenomenex Luna 250 mm × 4.60 mm) operating at 300 nm and run isocratically with acetonitrile:water (75:25).

Cell Culture and Proliferation Assay. Cell lines derived from human nonsmall cell lung cancers were obtained from American Type Culture Collection (ATCC, Manassas, VA) and are designated by their NCI numbers. Cells were maintained in RPMI 1640 medium (Gibco, Invitrogen, Carlsbad, CA), supplemented with 10% fetal calf serum (Gemini Bio-Products, Sacramento, CA), 100 U/mL penicillin/streptomycin, and 2 mM glutamine at 37 °C and 5% CO$_2$.

For proliferation assays, cells were seeded at 2 × 10^4 /well in 96-well plates, allowed to adhere for 24 h, and then were treated with the drug or DMSO as a control for 48 h. Final concentration of DMSO did not exceed 0.1%. Compounds were prepared as 10 mM stock solution in DMSO (Sigma, St. Louis, MO). Increasing drug concentrations in 10 μL of phosphate-buffered saline (PBS) were

added to 100 μL of the culture medium and incubated at 37 °C for 72 h. The CellTiter 96 nonradioactive cell proliferation assay (MTT assay, Promega, Madison, WI) was performed according to the manufacturer's protocol. Each compound concentration was represented in six repeats, and the screening was performed as at least two independent experiments. IC_{50} values were calculated using Sigma Plot software (Systat Software).

In Vivo Treatments. All animals used in this research project were cared for and used humanely according to the following policies: *The U.S. Public Health Service Policy on Humane Care and Use of Animals*, 1996; the *Guide for the Care and Use of Laboratory Animals*, 1996; and the U.S. Government *Principles for Utilization and Care of Vertebrate Animals Used in Testing, Research, and Training*, 1985. All NCI-Frederick animal facilities and the animal program are accredited by the Association for Assessment and Accreditation of Laboratory Animal Care International.

H1703 cells were harvested at 80% confluence, washed with PBS, and suspended in PBS. The cells were injected at 5×10^6 sc into a flank of 7-week-old female athymic NCr-nu/nu mice (Charles River). The drug injections were initiated when the tumors reached at least 2 mm × 2 mm × 2 mm (typically 4 weeks). Animals were treated three times a week for three weeks with iv tail vein injections of either vehicle (2.25% P-123 in PBS) or **1** or **2** (6 μmol/kg in the vehicle) or **6** (8 μmol/kg). Body weights were measured before each drug injection. Animals were sacrificed two hours after the last drug injection, and the tumors were excised and weighed. There were 13–15 mice/group at termination. The nonparametric Mann–Whitney test was utilized for statistical comparisons of tumor weights.

Treatment with siRNA. H1703 cells growing on 6-well plates at 60% confluence were transfected with siRNA to ATF3 (Santa Cruz Biotechnology, Santa Cruz, CA) or AllStars nonsilencing siRNA control (Qiagen, Valencia, CA), using HiPerfect transfection reagent (Qiagen). After 48 h, cells were treated with 1 μM compound **1** or equal volume of DMSO for 8 h, and then lysed and processed for immunoblotting.

Immunoblotting and Immunohistochemistry. Western blot analysis was performed as previously described.[22] Primary antibodies for caspases 3, 7, PARP, P-SEK1/MMK4, P-SAPK/JNK and SAPK/JNK, P-ATF2, P-c-jun (Cell Signaling Technology, Danvers, MA), cleaved PARP p85 (Promega, Madison, WI), and ATF3 (Santa Cruz Biotechnology, Santa Cruz, CA) were used. SAPK/JNK inhibitor 1,9-pyrazoloanthrone was obtained from Calbiochem, EMD Chemicals, San Diego, CA.

Paraffin-embedded xenograft tumor sections were analyzed for P-SAPK/JNK and ATF3 by immunohistochemistry using the antibody against P-SAPK/JNK (Cell Signaling, no. 4668) or ATF3 (Novus Biologicals, NBP1–02935). The staining intensity of the cells was categorized as negative (−), very weak (∓), weak (+), moderate (++), or strong (+++).

RT-PCR Analysis of ATF3 mRNA Expression. Total RNA from H1703 cells treated with **1** or DMSO control was isolated using RNeasy Mini kit (Qiagen, Valencia, CA). Residual genomic DNA was removed using DNA-free kit (Ambion/Applied Biosystems, Austin, TX). For ATF3 mRNA analysis, cDNA was synthesized using the SuperScript III Reverse Transcriptase kit (Invitrogen, Carlsbad, CA). TaqMan probes (Applied Biosystems, Foster City, CA) were used for real-time PCR amplification. The relative abundance of ATF3 transcript was normalized with β-actin internal control.

FACS Analysis. For flow cytometric (fluorescence-activated cell sorter [FACS]) analysis cells were treated with 1 μM compound **1** for 6 h, trypsinized, washed twice with ice-cold PBS, resuspended in PBS, fixed by the addition of absolute ethanol to a final concentration of 70%, and held at −20 °C. Two hours before the FACS analysis, the cells were washed with PBS and resuspended in PBS, and the cell nuclei were stained in the dark with 100 μg/mL propidium iodide (Sigma, St. Louis, MO) containing 125 U/mL RNase. Ten thousand stained nuclei were analyzed on a BD FACSCanto II using BD FACS DIVA software from Becton Dickinson Immunocytometry Systems, San Jose, CA. The cell cycle analysis was done using ModFit LT from Verity House Software, Inc., Topsham, ME.

Statistical Analysis. All experiments were performed at least three times, each time at least in triplicate. Results are presented as averages ± SE. Statistical tests were carried out using GraphPad Instat version 3.00 (GraphPad Software). Pairwise comparisons included the *t* test, with the Welch correction or application of the Mann–Whitney test as appropriate. Significance of correlations was assessed by the Pearson linear correlation or the Spearman test as appropriate.

■ ASSOCIATED CONTENT

Ⓢ Supporting Information

Results from elemental analysis; decomposition of compound **6** with GSH; immunohistochemical analysis of xenograft tumors. This material is available free of charge via the Internet at http://pubs.acs.org.

■ AUTHOR INFORMATION

Corresponding Author
*Phone: 301-846-1246. Fax: 301-846-5946. E-mail: maciaga@mail.nih.gov.

Author Contributions
#A.E.M. and R.S.N. contributed equally to this work.

■ ACKNOWLEDGMENTS

■ ABBREVIATIONS USED

NO, nitric oxide; JS-K, O^2-(2,4-dinitrophenyl) 1-[(4-ethoxycarbonyl)piperazin-1-yl]diazen-1-ium-1,2-diolate; NSCLC, nonsmall cell lung cancer; GST, glutathione *S*-transferase; GSH, glutathione; DFM-FM diacetate, 4-amino-5-methylamino-2′,7′-difluorofluorescein diacetate; DMSO, dimethyl sulfoxide; HBSS, Hanks's balanced salt solution; TBS-T, Tris-buffered saline-Tween-20; PBS, phosphate buffered saline; MTT, 3-(4,5-dimethylthiazol- 2-yl)-2,5-diphenyltetrazolium bromide

■ REFERENCES

(1) Schiller, J. H.; Harrington, D.; Belani, C. P.; Langer, C.; Sandler, A.; Krook, J.; Zhu, J.; Johnson, D. H. Comparison of four chemotherapy regimens for advanced non-small-cell lung cancer. *New Engl. J. Med.* **2002**, *346*, 92–98.

(2) Shami, P. J.; Saavedra, J. E.; Wang, L. Y.; Bonifant, C. L.; Diwan, B. A.; Singh, S. V.; Gu, Y.; Fox, S. D.; Buzard, G. S.; Citro, M. L.; Waterhouse, D. J.; Davies, K. M.; Ji, X.; Keefer, L. K. JS-K, a glutathione/glutathione *S*-transferase-activated nitric oxide donor of the diazeniumdiolate class with potent antineoplastic activity. *Mol. Cancer Ther.* **2003**, *2*, 409–417.

(3) Shami, P. J.; Saavedra, J. E.; Bonifant, C. L.; Chu, J.; Udupi, V.; Malaviya, S.; Carr, B. I.; Kar, S.; Wang, M.; Jia, L.; Ji, X.; Keefer, L. K. Antitumor activity of JS-K [O^2-(2,4-dinitrophenyl) 1-[(4-ethoxycarbonyl)piperazin-1-yl]diazen-1-ium-1,2-diolate] and related O^2-aryl diazeniumdiolates in vitro and in vivo. *J. Med. Chem.* **2006**, *49*, 4356–4366.

(4) Ren, Z.; Kar, S.; Wang, Z.; Wang, M.; Saavedra, J. E.; Carr, B. I. JS-K, a novel non-ionic diazeniumdiolate derivative, inhibits Hep 3B hepatoma cell growth and induces c-Jun phosphorylation via multiple MAP kinase pathways. *J. Cell. Physiol.* **2003**, *197*, 426−434.

(5) Kiziltepe, T.; Hideshima, T.; Ishitsuka, K.; Ocio, E. M.; Raje, N.; Catley, L.; Li, C. Q.; Trudel, L. J.; Yasui, H.; Vallet, S.; Kutok, J. L.; Chauhan, D.; Mitsiades, C. S.; Saavedra, J. E.; Wogan, G. N.; Keefer, L. K.; Shami, P. J.; Anderson, K. C. JS-K, a GST-activated nitric oxide generator, induces DNA double-strand breaks, activates DNA damage response pathways, and induces apoptosis in vitro and in vivo in human multiple myeloma cells. *Blood* **2007**, *110*, 709−718.

(6) Maciag, A. E.; Chakrapani, H.; Saavedra, J. E.; Morris, N. L.; Holland, R. J.; Kosak, K. M.; Shami, P. J.; Anderson, L. M.; Keefer, L. K. The nitric oxide prodrug JS-K is effective against non-small cell lung cancer cells in vitro and in vivo: involvement of reactive oxygen species. *J. Pharmacol. Exp. Ther.* **2011**, *336*, 313−320.

(7) Chakrapani, H.; Kalathur, R. C.; Maciag, A. E.; Citro, M. L.; Ji, X.; Keefer, L. K.; Saavedra, J. E. Synthesis, mechanistic studies, and anti-proliferative activity of glutathione/glutathione *S*-transferase-activated nitric oxide prodrugs. *Bioorg. Med. Chem.* **2008**, *16*, 9764−9771.

(8) Saavedra, J. E.; Srinivasan, A.; Bonifant, C. L.; Chu, J.; Shanklin, A. P.; Flippen-Anderson, J. L.; Rice, W. G.; Turpin, J. A.; Davies, K. M.; Keefer, L. K. The secondary amine/nitric oxide complex ion $R_2N[N(O)NO]^-$ as nucleophile and leaving group in S_NAr reactions. *J. Org. Chem.* **2001**, *66*, 3090−3098.

(9) Matsui, K.; Soeda, Y.; Otaguro, K.; Kuroda, T. Halobenzene reactive dyes. VII. Synthesis and reactivity of primary condensation products of 1,3-difluoro-4,6-dinitrobenzene. *Kogyo Kagaku Zasshi* **1965**, *68*, 507−511.

(10) Tournier, C.; Hess, P.; Yang, D. D.; Xu, J.; Turner, T. K.; Nimnual, A.; Bar-Sagi, D.; Jones, S. N.; Flavell, R. A.; Davis, R. J. Requirement of JNK for stress-induced activation of the cytochrome c-mediated death pathway. *Science* **2000**, *288*, 870−874.

(11) Papadakis, E. S.; Finegan, K. G.; Wang, X.; Robinson, A. C.; Guo, C.; Kayahara, M.; Tournier, C. The regulation of Bax by c-Jun N-terminal protein kinase (JNK) is a prerequisite to the mitochondrial-induced apoptotic pathway. *FEBS Lett.* **2006**, *580*, 1320−1326.

(12) Hai, T.; Hartman, M. G. The molecular biology and nomenclature of the activating transcription factor/cAMP responsive element binding family of transcription factors: activating transcription factor proteins and homeostasis. *Gene* **2001**, *273*, 1−11.

(13) Yan, C.; Lu, D.; Hai, T.; Boyd, D. D. Activating transcription factor 3, a stress sensor, activates p53 by blocking its ubiquitination. *EMBO J.* **2005**, *24*, 2425−2435.

(14) Hartman, M. G.; Lu, D.; Kim, M. L.; Kociba, G. J.; Shukri, T.; Buteau, J.; Wang, X.; Frankel, W. L.; Guttridge, D.; Prentki, M.; Grey, S. T.; Ron, D.; Hai, T. Role for activating transcription factor 3 in stress-induced beta-cell apoptosis. *Mol. Cell. Biol.* **2004**, *24*, 5721−5732.

(15) Syed, V.; Mukherjee, K.; Lyons-Weiler, J.; Lau, K. M.; Mashima, T.; Tsuruo, T.; Ho, S. M. Identification of ATF-3, caveolin-1, DLC-1, and NM23-H2 as putative antitumorigenic, progesterone-regulated genes for ovarian cancer cells by gene profiling. *Oncogene* **2005**, *24*, 1774−1787.

(16) Mashima, T.; Udagawa, S.; Tsuruo, T. Involvement of transcriptional repressor ATF3 in acceleration of caspase protease activation during DNA damaging agent-induced apoptosis. *J. Cell. Physiol.* **2001**, *188*, 352−358.

(17) Cai, Y.; Zhang, C.; Nawa, T.; Aso, T.; Tanaka, M.; Oshiro, S.; Ichijo, H.; Kitajima, S. Homocysteine-responsive ATF3 gene expression in human vascular endothelial cells: activation of c-Jun NH_2-terminal kinase and promoter response element. *Blood* **2000**, *96*, 2140−2148.

(18) Lu, D.; Wolfgang, C. D.; Hai, T. Activating transcription factor 3, a stress-inducible gene, suppresses Ras-stimulated tumorigenesis. *J. Biol. Chem.* **2006**, *281*, 10473−10481.

(19) Turchi, L.; Aberdam, E.; Mazure, N.; Pouyssegur, J.; Deckert, M.; Kitajima, S.; Aberdam, D.; Virolle, T. Hif-2alpha mediates UV-induced apoptosis through a novel ATF3-dependent death pathway. *Cell Death Differ.* **2008**, *15*, 1472−1480.

(20) Bhoumik, A.; Fichtman, B.; Derossi, C.; Breitwieser, W.; Kluger, H. M.; Davis, S.; Subtil, A.; Meltzer, P.; Krajewski, S.; Jones, N.; Ronai, Z. Suppressor role of activating transcription factor 2 (ATF2) in skin cancer. *Proc. Natl. Acad. Sci. U.S.A.* **2008**, *105*, 1674−1679.

(21) Chen, S. C.; Liu, Y. C.; Shyu, K. G.; Wang, D. L. Acute hypoxia to endothelial cells induces activating transcription factor 3 (ATF3) expression that is mediated via nitric oxide. *Atherosclerosis* **2008**, *201*, 281−288.

(22) Romanowska, M.; Maciag, A.; Smith, A. L.; Fields, J. R.; Fornwald, L. W.; Kikawa, K. D.; Kasprzak, K. S.; Anderson, L. M. DNA damage, superoxide, and mutant K-ras in human lung adenocarcinoma cells. *Free Radical Biol. Med.* **2007**, *43*, 1145−1155.